Identification of Wildfire Burn Areas in Eastern Washington Using Satellite Remote Sensing

Tufts University School of Engineering

Poster & Cartography by Matthew Simon

Projection: NAD 1983 HARN State Plane Washington South FIPS 4602

Introduction

Forest fires have been increasing in severity and frequency in recent years in the western United States.[1] The fire itself poses many problems, such as property and vegetation damage and increases in local air pollution levels,[2] but post-fire concerns are not trivial. Determining the best watershed treatment, minimizing erosion effects, and monitoring habitat rehabilitation are of great importance. Remote sensing is a powerful tool used that can be used for this purpose.[3] Using satellites, it is possible to map the regions that have been burned and determine burn severity using ratios of different spectral bands, such as the Normalized Burn Ratio (NBR) or differenced NBR.[4-6] Classification tools, such as those provided by the Exelis Visual Information Solutions (ENVI) software, can also be used to help identify burn sites.[4] These tools may help in instances where burn sites closely resemble natural (arid) land.[6]

Objectives

The goal of this project is to evaluate the use of supervised classification in identifying wildfire burn sites in locations where it may be difficult to distinguish between desert and burnt land. It is hypothesized there will be a significant amount of noise in the classification models unless limits are placed on the classification tool and its identification of burn sites, and the more interpretable model (visually) may not align with the "best" model according to the confusion matrix. The specific objectives of this project are:

1. Develop three classification models for identifying wildfire burn sites.
2. Analyze model performance and signal-to-noise ratios for each model.

Methodology

A Landsat 8 OLI/TIRS surface reflectance image for eastern Washington was acquired from the U.S. Geological Survey (Fig. 1). The image was captured on Sept. 1, 2014 at 11:49 PDT and included a mix of forested, desert, and agricultural land areas. GIS shapefiles of known wildfire perimeters were acquired from the Northwest Interagency Coordination Center. Normalized Burn Ratios (NBR) were calculated based on the following equation: *NBR = (NIR-MIR)/(NIR+MIR)* (Fig 2). All seven spectral bands and two NBR were used for supervised classification (i.e., Maximum Likelihood). Nine classes were created, including a Burn Site class.

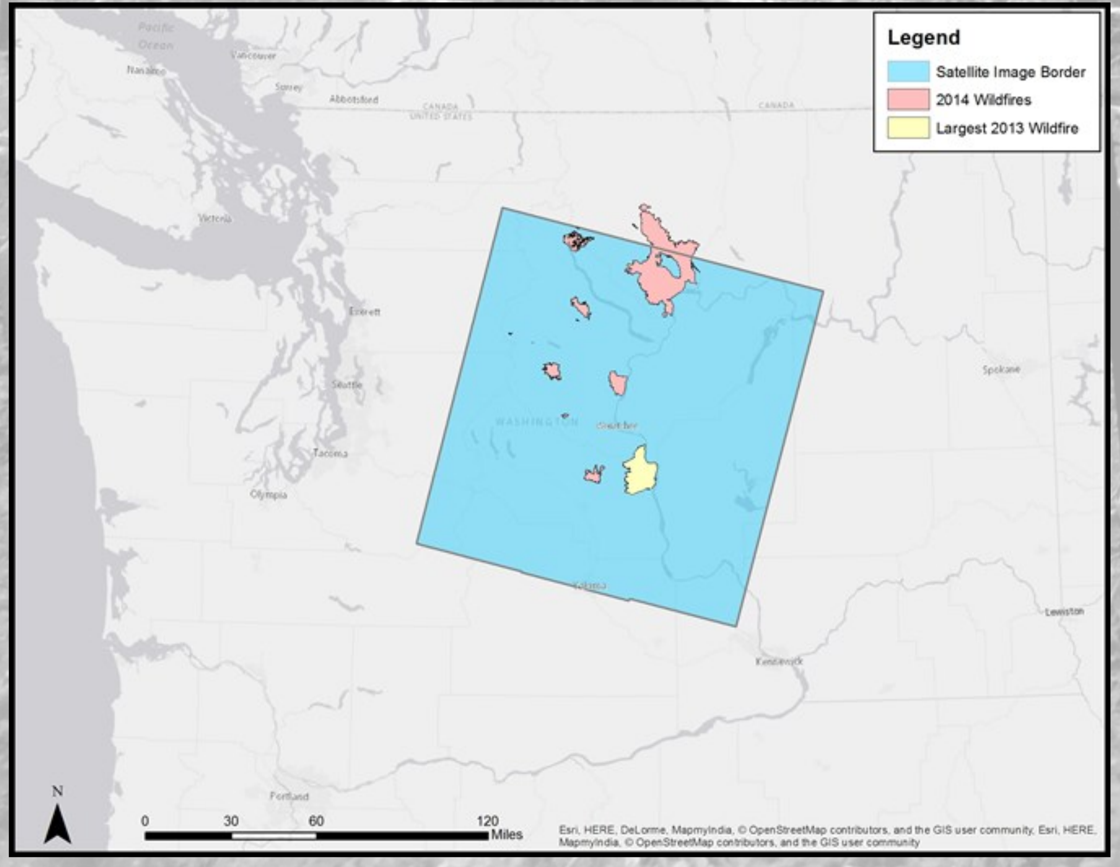

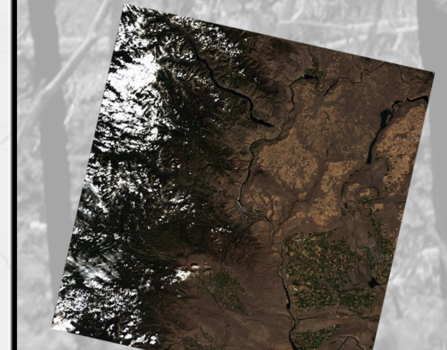

Fig. 1: (left) Map of satellite image area (blue) used for analysis, relative to Washington. Wildfires shown are those used for analysis, although, these are not the only wildfires from 2013 or 2014. (below) Natural color image from September 1, 2014 used for analysis.

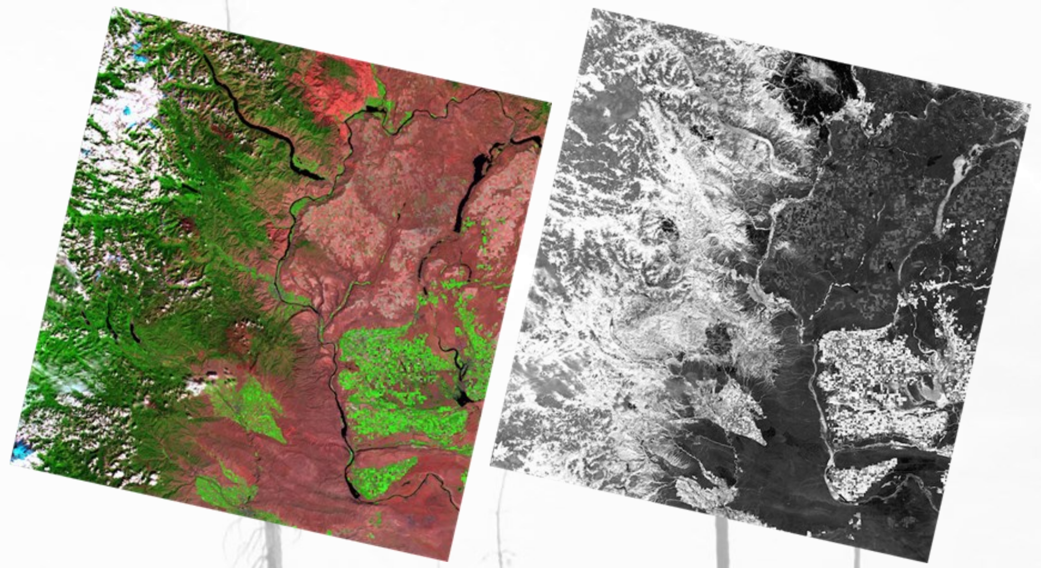

Fig. 2: False color image using Landsat 8 bands: R = 7, G = 5, B = 4 (left) and NBR image using Landsat 8 bands 5 and 7 for NIR and MIR, respectively (right). Darkest areas in NBR image represent burn sites.

Results

Three different classification models were developed using the Maximum Likelihood supervised classification tool in ENVI (Fig. 3-5). All models are identical except for the lower probability limit (LPL) assigned to the Burn Site class. Model 1 has an LPL = 0.00, Model 2 has an LPL = 0.05, and Model 3 has an LPL = 0.50. Tables 1 and 2 provide details on the models' performance. Table 3 provides additional details on the performance of the classification models, except for the Burn Site class, which is shown in Table 1.

Table 1: Results from confusion matrix for each of the three classification models, as well as a signal-to-noise ratio.

	Model 1 (LPL = 0.00)	Model 2 (LPL = 0.05)	Model 3 (LPL = 0.50)
Misclassification Rate (CI)	0.1146 (0.1137, 0.1154)	0.1229 (0.1221, 0.1238)	0.1518 (0.1508, 0.1527)
Kappa coefficient	0.8423	0.8313	0.7934
Burn Site Producer Accuracy (%)	76.46	71.59	54.75
Burn Site User Accuracy (%)	87.41	88.49	91.11
Signal-to-Noise Ratio	0.185	0.305	0.594

Table 2: Percentage of identified wildfire regions classified correctly.

Wildfire Region	Model 1 (LPL = 0.00)	Model 2 (LPL = 0.05)	Model 3 (LPL = 0.50)
Carlton	84.7	65.1	31.8
Chiwaukum	70.2	45.1	18.3
Colockum Tarps*	30.3	23.0	8.72
Lone Mtn. 1	40.3	10.3	1.20
Mills Canyon	76.5	71.6	54.8
Snag Canyon	85.1	76.1	51.3

* Largest wildfire (area) in the satellite field of view from 2013.

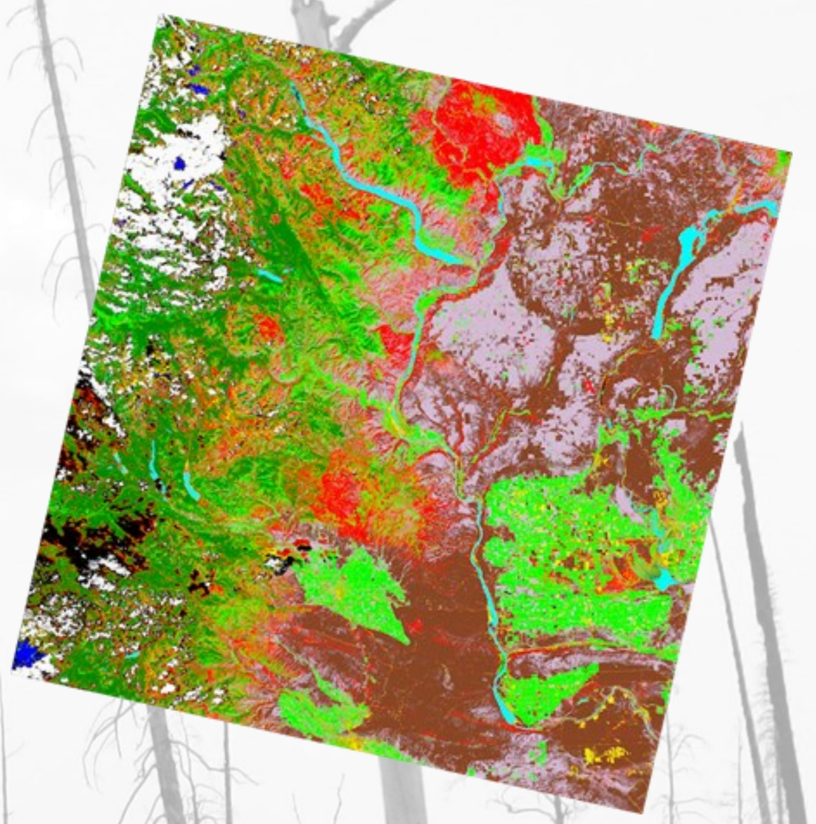

Fig. 3: Classification model 1; Lower Probability Limit (LPL = 0.00). Red represents the Burn Site class.

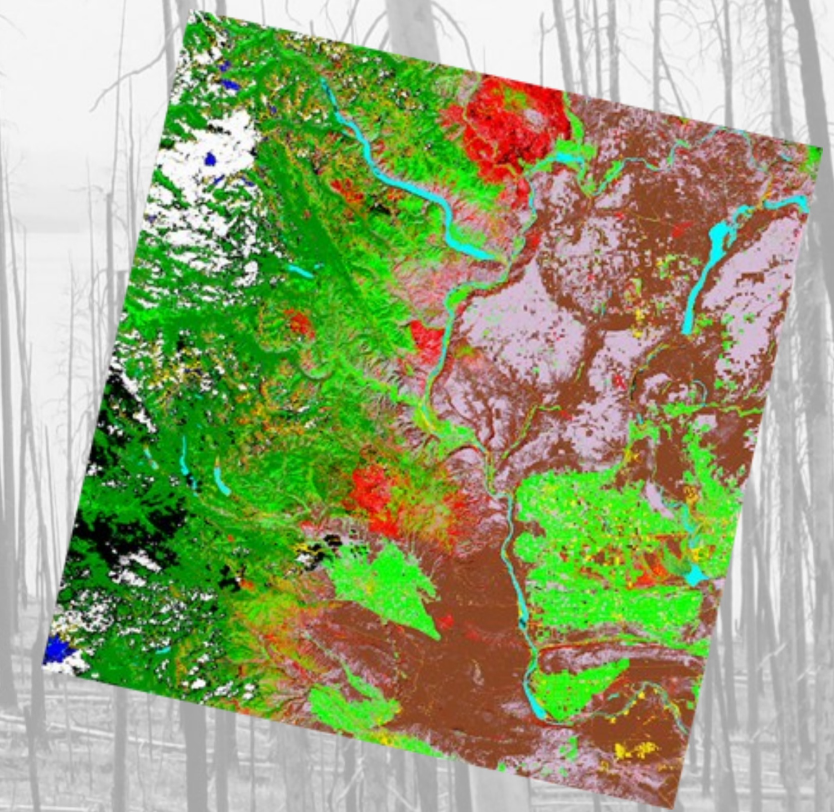

Fig. 4: Classification model 2; Lower Probability Limit (LPL) = 0.05. Red represents the Burn Site class.

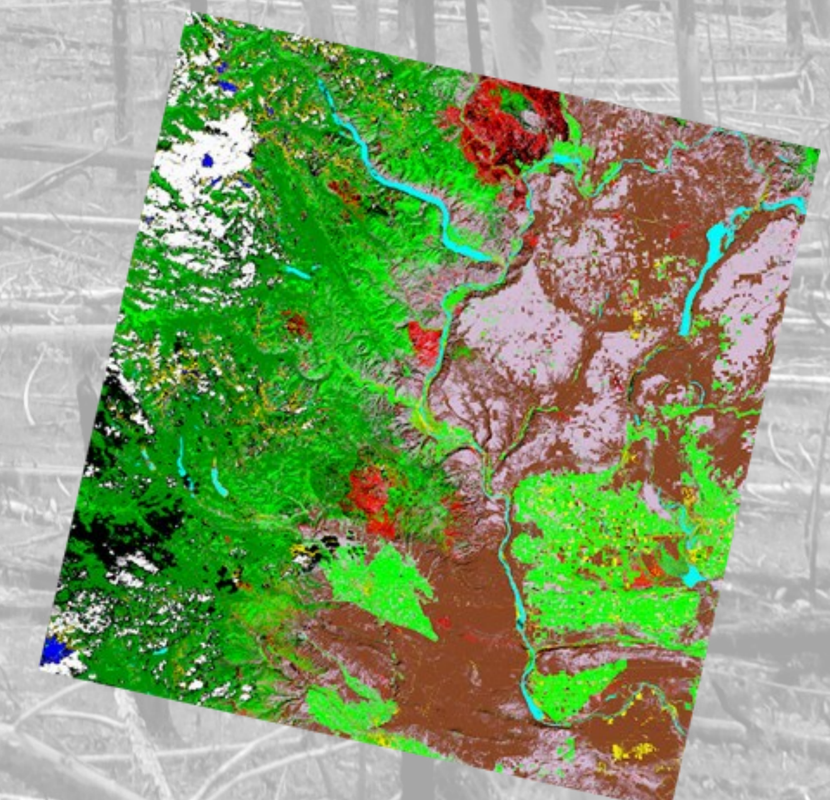

Fig. 5: Classification model 3; Lower Probability Limit (LPL) = 0.50. Red represents Burn Site class.

Table 3: Producer accuracy and user accuracy for all classes, except Burn Site, for all three models.

Class	Color Key	Producer Accuracy (%)	User Accuracy (%)
Crops	Bright Green	96.96	82.16
Natural Vegetation	Dark Green	98.44	98.00
Desert	Dark Brown	92.13	88.44
Dry Cropland	Light Brown	84.92	87.35
Snow/Ice	Blue	99.92	100.0
Clouds	White	99.95	99.99
Urban Area	Yellow	79.11	54.05
Water	Cyan	99.66	100.0
Undefined	Black	N/A	N/A

Conclusions

1. Application of classification models for use in identifying wildfire burn sites seems promising and may prove easier to interpret than Normalized Burn Ratios or false color images.
2. Model 1 appears to be the best based on classification performance metrics (i.e., confusion matrix), but Model 3 performs best when including visual interpretability (e.g., signal-to-noise ratio).
3. The human factor is hugely important in determining how well these models perform. Signal-to-noise ratio is the closest quantitative metric available to measure this.
4. Additional time would likely result in a model with a lower misclassification rate and a higher signal-to-noise ratio.

References

1. Miller et al., 2009, Remote Sensing of Environment, 113(3), 645-656.
2. Langmann et al., 2009, Atmospheric Environment, 43, 107-116.
3. Miller et al., 2002, Remote Sensing of Environment, 82(2-3), 481-496.
4. Rogan et al., 2001, Geocarto International, 16(4), 91-106.
5. Roy et al., 2006, Geo. & Remote Sensing Letters, ISEE, 3(1), 112-116.
6. Sundermann et al., 2011, Remote Sensing of Env., 115(9), 2384-2389.
7. Escuin et al., 2008, Int. Journal of Remote Sensing, 29(4), 1053-1073.

Acknowledgements

I am grateful to Alex Liss and Madeline Wrable who provided guidance on this project. Poster background photo was obtained online at: http://residentalien.co/2013/06/19/yellowstone-do-over-part-4-trees. Landsat 8 Surface Reflectance images were downloaded from USGS. Fire perimeter shapefiles were downloaded from the Northwest Interagency Coordination Center website. Maps were created using ArcGIS® software by Esri. ArcGIS® and ArcMap™ are the intellectual property of Esri and are used herein under license. For more information about Esri® software, please visit www.esri.com. Additional data analyses were done using ENVI version 5 (Exelis Visual Information Solutions, Boulder, Colorado).